

Molecular Docking Analysis of Christanoate and Christene from *Christia vespertilionis* Plants as Potential Inhibitors of Covid-19

Suganya Murugesu¹, Tavamani Balan¹, Nurliyana Ismahani Mohd Tamri¹,
Lukhman Nul Hakim Zamree¹, Nurul Fathiah Zulkifli Samba¹, Siti Nur Hajar
Mohamed Anuar¹, Sharon Fatinathan¹, Vikneswari Perumal¹

¹Faculty of Pharmacy and Health Sciences, Royal College of Medicine Perak, Universiti Kuala Lumpur, 30450 Ipoh, Perak, Malaysia.

Corresponding author: vikneswari@unikl.edu.my

Abstract

Covid-19 is a global pandemic caused by SARS-CoV-2 virus that caused mortality and world economic collapse. It is almost impossible to break the chain of infection with no intervention except vaccines to prevent worsening symptoms and to build herd immunity in people. Efforts to discover a therapeutic drug to combat the virus are still ongoing. Various medicinal phytoconstituents are also researched for their pharmacological action as antiviral agents against Covid-19. This study explored the antiviral potential of *Christia vespertilionis* bioactive compounds (christene and christanoate) for treating Covid-19 using molecular docking analysis. The Covid-19 protein crystal structures (PDB ID: 6LU7, PDB ID: 6CS2, PDB ID: M1D, PDB ID: 2GHV and PDB ID: 6M71) obtained from the protein data bank were docked to christene and christanoate. The analyses were carried out using the Autodock tool 1.5.6. The control docking was done using favipiravir as the reference drug. The binding interaction of the protein and ligand was observed using the Biovia Discovery visualizer. The binding affinity and interactions indicate that the observed compounds have antiviral action suggesting their potential as Covid-19 inhibitors and can be further considered for therapeutic applications.

Keywords: SARS-CoV-2, *Christia vespertilionis*, molecular docking, Covid-19

Introduction

The outbreak of coronavirus disease (COVID-19) caused a global health emergency at the end of 2019 (1). The RNA virus has caused significant economic and social repercussions providing a significant threat globally (2). According to Chen et al., (3), the virus was most likely transmitted to humans through infected droplets from bats. The majority of those infected with COVID-19 will experience mild to moderate respiratory symptoms and will recover without the need for additional treatment. However, COVID-19 can develop serious illnesses in older people, those suffering from medical conditions such as heart disease, diabetes, chronic pulmonary illness, and cancer. Currently, vaccination has been approved for mass immunization. However, there is decreasing vaccine coverage and an increasing risk of vaccine-preventable disease outbreaks and epidemics due to vaccine hesitancy. Vaccination is perceived as unnecessary by many individuals due to their belief, lack of confidence, and presumed unsafe (4). The key goals to fight against the rapidly evolving virus are developing new therapies or repurposing drugs (5,6).

The SARS-CoV-2 virus belongs to the Coronaviridae family, subfamily coronavirinae and Nidovirales order. It is a protein-sense RNA virus with a single linear RNA segment on a sin-

gle strand. SARS-CoV-2 is a member of Sarbecovirus, which undergo frequent recombination. If there are enough sequenced genomes, building a phylogenetic tree of a virus family's mutation history is possible. The China Centre for Disease Control and Prevention reported five SARS-CoV-2 genomes isolated from Wuhan in early 2020 (7). At the epicentre of the pandemic in Wuhan, SARS-CoV-2 was treated with favipiravir, a therapeutic drug approved for emergency use in Italy as the pandemic expanded through Europe, and it is currently being used in Japan, Russia, Ukraine, Uzbekistan, and Kazakhstan. Favipiravir is a synthetic prodrug found while evaluating the antiviral effectiveness of chemical compounds used to treat influenza strain (A/PR/8/34-H1N1), later identified as T1105. Favipiravir has high bioavailability, protein binding affinity and small distribution volume. It reaches maximum concentration within 2 hours after a single dose. It has a short half-life of 2.5 to 5 hours, leading to rapid renal elimination in the hydroxylated form. Elimination is mediated by aldehyde oxidase and marginally by xanthine oxidase. The pharmacokinetics of favipiravir is dose-dependent as well as time-dependent. The cytochrome P450 system does not metabolize it but blocks one of its components (CYP2C8). As a result, it should be used with caution when coupled with drugs metabolized by the CYP2C8 system (8).

In recent decades, research on the use of medicinal plants for various pharmacological actions has been carried out vastly. Secondary metabolites from plants, such as flavonoids, have been shown to have tremendous bioactivities, including antiviral effects. *Christia vespertilionis* (L.f.) Bakh. F. is an ornamental plant in the Fabaceae family. It is also known as mariposa or butterfly wing for its distinctive trifoliate leaf shape. *C. vespertilionis* is a species native to Southeast Asia and Brazil. This plant has traditionally been used to treat snake bites and facilitate healing in respiratory and tuberculosis cases (9). Furthermore, *C. vespertilionis* is used to treat muscle fatigue, colds, inflamed tonsils, impaired blood circulation, and inflamed bronchi-

tis and to increase blood circulation. According to Bunawan et al., (10), *C. vespertilionis* can treat many diseases and is a viable alternative to modern synthetic medicines. The plant was previously reported to possess antidiabetic activity (11), anti-tumour and antiproliferative activities (12), followed by antimalarial activity (13). Upadhyay et al., (13) reported on the antiplasmodial and antimalarial activities of *C. vespertilionis* roots, leaves, and stems methanolic extracts using *in vitro* and animal model assays. Their study revealed two potential compounds, namely christene and christanoate, with more pharmacological activity to be explored (13,14).

Therefore, this study uses molecular docking analysis to investigate the Covid-19 protein-inhibiting activity of christene and christanoate from *C. vespertilionis*. About five protein structures (PDB ID: 6LU7, PDB ID: 6CS2, PDB ID: 6M1D, PDB ID: 2GHV and PDB ID: 6M71) related to the Covid-19 protein sequence were selected for the analysis.

Materials & methods

Preparation of ligands

A 3D model of the identified compound was constructed using Chem3D software. The structures and formal charges of the targeted compound were checked through 2D drawing (Fig. 1) and subjected to conformational research. Energy minimization was set on all conformers, and the partial charges were automatically calculated. The data obtained was saved in the MDB file for further docking studies.

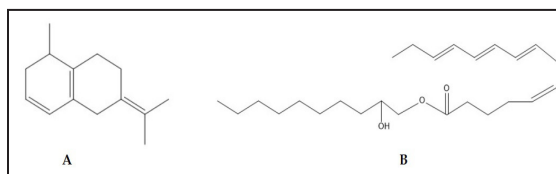


Fig 1. A: Christene (7-isopropylidene-1-methyl-2,6,7,8,9-hexahydronaphthalene) and B: Christanoate (2'-hydroxydecanylpentadec-5,8,10,12-tetraenoate) from *Christia vespertilionis* leaf

Optimization of the enzyme active site

The X-ray crystallographic structure of the proteins displayed in **Fig. 2** (PDB ID: 6LU7, PDB ID: 6CS2, PDB ID: 6M1D, PDB ID: 2GHV and PDB ID: 6M71) was obtained from the Protein Data Bank at <https://www.rcsb.org>. Hydrogen atoms were added to stabilize the charges of the proteins in their respective standard geometry form. To check errors in atom's type and connection, automatic correction was applied to ease the process. The receptor was selected, and its atom's potential was fixed. All default items were used to search the active site in each enzyme structure with the site finder. The site finder of the pocket was used to create dummy atoms on the enzymes.

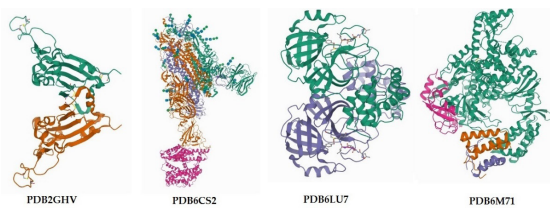


Fig 2. The protein structure of SARS-CoV-2; PDB ID: 2GHV, PDB ID: 6LU7, PDB ID: 6CS2, PDB ID: 6M1D, and PDB ID: 6M71

Docking analysis

The docking process between christene and christanoate with the proteins was conducted using AutoDock Tools by uploading the enzyme's active site in PDB file format. Dummy atoms were added and adjusted on the docking site with the program specifications. The active binding site between the ligand and receptor was placed in the centre of the grid box. The grid box size was adjusted up to 126x126x126 to cover all binding sites involved. It was used to calculate the interaction energies between the ligand-receptor interactions. The AutoDock was used to calculate the docking automatically, and each compound's lowest binding energy was selected. The process preceded the study of the illustration of the ligand-receptor interaction in both 2D and 3D structures on the Discovery Studio Visualizer.

The rotatable bonds were set with AutoDockTools, and all torsions can be rotated. Ligand protein tethering was accomplished by adjusting the genetic algorithm (GA) parameters throughout ten runs of the GA criteria. Gasteiger charges were added by default. The maximum grid box size was used with the default spacing. The grid box parameters for X, Y, and Z centres were 142.5142, 131.9530 and 177.2277, respectively. Molecular dynamics (MD) simulations were then applied to multiple conformations of the 6M1D-christanoate complexes. For each compound, the highest-scoring docking poses were selected. Autodock 4.2 and BIOVIA Discovery Studio Visualizer 2021 analyzed the protein-ligand complexes with the lowest binding energy.

Results and Discussion

All the results are tabulated below with the details on the residues and binding energy that represents the interaction between protein and compounds (christanoate and christene) observed. Based on the results obtained, the binding energy score of the compounds docked indicates the affinity of the compounds towards the protein and its binding site residues. The positive control used in this study is favipiravir prescribed to the Covid 19 patients. Table 1 displayed the interaction of christanoate and christene with the COVID-19 proteins.

PDB ID: 2GHV is the spike protein (S protein) of SARS-CoV targeting the angiotensin-converting enzyme 2 (ACE2) receptors. The positive control, favipiravir, was docked to the residues in Chain E of the receptor where Phe329, Asn330 and Ala331 interacted via hydrogen bonding and other conventional bonding with Thr332, Phe334, Tyr356, Asn357, Thr359, Trp423 and Arg495. The binding energy score of favipiravir was -5.4 kcal/mol, slightly lower than christine (-6.1 kcal/mol) and christanoate (-5.6 kcal/mol). Christene has made only hydrophobic interaction with the chain E residues, namely Arg441, Leu443, Arg444, His445, Asp454, Ser456, Val458, Pro459, Phe460, Ser461,

Table 1. The interaction of christanoate and christene with the COVID-19 proteins

Proteins (PDB)	Ligands	Hydrogen bond residues	Other residues	Binding affinity (Kcal/mol)
2GHV	favipiravir	Chain E: Phe329, Asn330, Ala331	Chain E: Thr332, Phe334, Tyr356, Asn357, Thr359, Trp423, Arg495	-5.4
	Christene	-	Chain E: Arg441, Leu443, Arg444, His445, Asp454, Ser456, Val458, Pro459, Phe460, Ser461, Lys465, Pro466, Cys467, Pro477	-6.1
	Christanoate	Chain E: Phe329, Arg495	Chain E: Asn330, Ala331, Thr332, Phe334, Tyr356, Asn357, Ser358, Thr359, Phe360, Phe361, Ser362, Trp423, Asn424, Thr425, Asn427, Ile428	-5.6
6LU7	favipiravir	Chain A: Phe8, Ile106, Phe112, Gln127, Asp153, Thr292	Chain A: Gln110, Thr111, Asn151, Phe294, Asp295	-5.4
	Christene	-	Chain A: Phe8, Val104, Ile106, Gln107, Gln110, Asn151, Asp153, Ser158, Phe294	-6.3
	Christanoate	Chain A: Leu141, Asn142, Gly143, Ser144, Cys145, His163	Chain A: Thr24, Thr25, Thr26, Leu27, His41, Met49, Tyr54, Phe140, His164, Met165, Glu166, His172, Asp187, Arg188, Gln189	-5.6
6CS2	favipiravir	Chain A: Lys1020 Chain B: Glu1013, Lys1020, Arg1021	Chain A: Glu1013, Ser1019, Arg1021, Val1022 Chain B: Ser1019 Chain C: Glu1013, Arg1021	-6.0
	Christene	-	Chain B: Trp101, Ile116, Asn118, Val123, Arg183, Phe185, Phe187, Val196, Lys198, Ile219, Phe220	-7.5
	Christanoate	Chain A: Lys1020	Chain A: Trp868, Tyr886, Gly1017, Gln1018, Ser1019, Lys1020, Arg1021 Chain B: Glu1013, Lys1020, Arg1021 Chain C: Gln1018, Ser1019, Lys1020, Val1022, Tyr1029, Arg1089	-6.5
6M71	favipiravir	Chain A: Ser343, Asp358, Asn360, Tyr374, Tyr530	Chain A: Ile333, Val342, Thr344, Asn356, Val359, Glu370	-5.5
	Christene	-	Chain A: Arg33, Ala34, Phe35, Val71, Arg116, Lys121, Thr123, Asp126, Asp208, Tyr217, Asp218	-6.1
	Christanoate	Chain A: Asn138	Chain A: Tyr32, Lys47, Asp135, His133, Asp135, Cys139, Ala706, Ser709, Thr710, Gly774, Lys780, Asn781, Ser784	-4.7

Lys465, Pro466, Cys467 and Pro477. Meanwhile, christanoate formed hydrogen bonding with Phe329 and Arg495 and hydrophobic bond with Asn330, Ala331, Thr332, Phe334, Tyr356, Asn357, Ser358, Thr359, Phe360, Phe361, Ser362, Trp423, Asn424, Thr425, Asn427 and Ile428.

The second protein used in this *in silico* study was PDB ID: 6LU7, the main protease of SARS-CoV with chain A and B. All three ligands

interacted with the residues from chain A, indicating the potential inhibiting site. The control drug displayed hydrogen bonding with Phe8, Ile106, Phe112, Gln127, Asp153 and Thr292. Meanwhile, the residues bind through other hydrophobic bonding, including Gln110, Thr111, Asn151, Phe294 and Asp295. Christene displayed bonding with Phe8, Val104, Ile106, Gln107, Gln110, Asn151, Asp153, Ser158 and Phe294 in chain A via hydrophobic bond-

Christanoate and christene are potential inhibitors of Covid-19

ing. Meanwhile, residues from chain A namely Leu141, Asn142, Gly143, Ser144, Cys145 and His163 bind through hydrogen bonding and Thr24, Thr25, Thr26, Leu27, His41, Met49, Tyr54, Phe140, His164, Met165, Glu166, His172, Asp187, Arg188 and Gln189 bind via hydrophobic bonding with christanoate. These two ligands displayed better binding scores than the control (-5.4 kcal/mol) ligand, with binding energy levels of -6.3 and -5.6 kcal/mol.

The SARS-CoV spike glycoprotein with human ACE2 bound particles (PDB ID: 6CS2) was used to dock the two compounds of *C. vespertilionis* leaf. favipiravir, christene and christanoate displayed the lowest binding energy level among all the other receptors docked with the binding score value of -6.0, -7.5 and -6.5 kcal/mol, respectively. The control drug interacted with residues in chain A (Lys1020) and B (Glu1013, Lys1020, and Arg1021) and bound through hydrogen bonding. Meanwhile, Glu1013, Ser1019, Arg1021, and Val1022 from chain A, Ser1019 in chain B, followed by Glu1013 and Arg1021 in chain C, made hydrophobic bonding with favipiravir. Christene showed more affinity towards the residues in chain B involving Trp101, Ile116, Asn118, Val123, Arg183, Phe185, Phe187, Val196, Lys198, Ile219 and Phe220. However, Christanoate has shown binding with residues in all three chains, similar to the control drug. The compound made a hydrogen bond with Lys1020 in chain A. Other than that, it made hydrophobic bond with Trp868, Tyr886, Gly1017, Gln1018, Ser1019, Lys1020 and Arg1021 in chain A, followed by interaction with Glu1013, Lys1020 and Arg1021 in chain B and with Gln1018, Ser1019, Lys1020, Val1022, Tyr1029 and Arg1089 in chain C.

Lastly, the RNA-dependant RNA polymerase PDB ID: 6M71 was used in this study to determine the molecular affinity of the compounds observed against SARS-CoV. Christene (-6.1 kcal/mol) exhibited the highest binding energy score compared to christanoate (-4.7 kcal/mol) and favipiravir (-6.1 kcal/mol). favipiravir interacted with the residues in chain

A, including Ser343, Asp358, Asn360, Tyr374 and Tyr530 via hydrogen bond and with Ile333, Val342, Thr344, Asn356, Val359 and Glu370 via the hydrophobic bond. Christene binds to Arg33, Ala34, Phe35, Val71, Arg116, Lys121, Thr123, Asp126, Asp208, Tyr217 and Asp218 in chain A via hydrophobic bonding. Meanwhile, christanoate interacted with Asn138 via hydrogen bonding followed Tyr32, Lys47, His133, Asp135, Cys139, Ala706, Ser709, Thr710, Gly774, Lys780, Asn781 and Ser784 via hydrophobic contact. Both the compounds were found to be interacting with residues in chain A, however, of different potential sites, unlike the control ligand.

The search for novel antiviral drugs targeting various parts of its structure to combat viral infection is ongoing. The current docking analysis using christene and christanoate from the *C. vespertilionis* leaf indicates that the compounds have a high affinity towards the proteins used in the docking analysis. Apart from the active site residues that alter the protein function, other residues that interacted with the compounds were also observed.

The structural details of the Coronavirus (SARS-CoV) genome were described by Wang et al., (15) as a single-stranded positive-sense RNA (+ssRNA) that is typically larger than other RNA viruses. It is packed with four structural proteins, namely spike protein (S1 and S2), membrane protein (M), envelope protein (E) and nucleoprotein (N). It contains non-structural proteins (NSP1-16), each with distinct functions in the evolution of the viral material. Some of the SARS-CoV proteins that can potentially serve as the therapeutic drugs target include the spike glycoprotein and its binding domain, the RNA-dependent RNA polymerase (RdRp) complex and the main protease (Mpro) (15).

The most vulnerable receptor during SARS-CoV infection is the ACE2 receptor of the host cell. PDB ID: 2GHV is the sequenced spike protein (S protein) of SARS-CoV that tar-

gets the ACE2 receptors in the host, making it a possible therapeutic target for the treatment. Typically, the virus is named coronavirus based on its crown-like shape resembling the trimeric form that the virion takes upon S protein interaction (16). Christene has shown significant binding score towards the spike protein. However, christanoate showed interaction with the residues (Phe329 and Arg495) similar to that of the control drug, favipiravir, thus indicating its target site is similar to the drug and may potentially forbid the interaction of the spike protein with the host cell. Changes in the structural conformation of the protein observed may have contributed to the inhibition of the protein activity (17).

The main protease-Mpro structure plays a crucial role in the viral's proteolytic maturation; thus, its inhibition may interrupt the life cycle (18). Based on the conformational complex of the main protease-Mpro (PDB ID: 6LU7) with the potential inhibitors showed that christanoate has a high affinity towards residues intact in the active site and the catalytic dyad of the protein reported by Khaerunnisa et al., (19). The active site residues of the protein include Thr24, Thr26, Phe140, Asn142, Gly143, Cys145, His163, His164, Glu166 and His172. Paasche et al., (20) in their investigation to find potential inhibitors of 3CLpro, have demonstrated the residues (His41 and Cys145) that define the catalytic dyad of the protein interacted with the inhibitors used. Catalytic dyads indicate sites with residues vital for the catalytic activity of the protein. The docking of favipiravir, christene and christanoate to this protein showed christanoate as the significant inhibitor as it interacted with the amino acids in the active site, and the catalytic dyad of the protein that included Cys145 and His163 interacted through hydrogen bonding; meanwhile, Thr24, Thr26, His41, Phe140, His164, Glu166, and His172 interacted via hydrophobic bonding. Christene displayed interaction similar to favipiravir, indicating its capacity to prevent protein activity. This inhibition pattern serves as evidence that an allosteric binding site may be present in the protein structure with

the ability to alter the activity of the protein (21). Favipiravir and christene were observed to bind with the amino acids near the active site pocket, blocking the entrance that may have altered the protein conformation, thus halting the viral activity.

These results are similar to that reported by Sisakht et al., (22), who used phytochemicals from various plant sources against 3CLpro. Ginkgolide M (Asn142, Cys145, Glu166, Gly143, His163, and Phe140), Glycobismine A (Ser144A, Cys145A, Gly143A, Leu141A, His163A, and Asn142A) and mezerein (His163A, Ser144A, Cys145A, Leu141a, Asn142, and Met49A) are the three compounds that displayed high affinity towards the residues in the catalytic site of the protease. Meanwhile, another study reported on luteolin interaction with the allosteric site, potentially inhibiting protein activity. The interaction involved Arg105, Gln110, Thr111 and Ile152 via hydrogen bonding and hydrophobic contact with Phe8, Arg105, Ile106, Gln107, Val104, Gln110, Thr111, Asn151, Ile152, Asp153, Thr292 and Phe294.

Another SARS-CoV spike glycoprotein with human ACE2-bound particles is deposited as PDB ID: 6CS2. Christanoate was observed to bind with the residues similar to the control drug with interaction in all three chains (A, B and C). Compared to christene, christanoate has more affinity towards the residues similar to favipiravir, with more hydrophobic contact rather than hydrogen bonding. The results are contrary to Sharbidre et al., (23) who displayed the interaction of an anti-inflammatory compound, bergenin, with the S-protein Lys715, Asp757, Leu843, Pro845, Asp849, Pro1039 and His1040. Pal and Talukdar (24) reported that the crucial residues of the S-protein active site include Lys26, Asn90 and Phe32. Another study reported potential catalytic sites of the protein involving Thr51, Leu52, Lys291, Ser292 and Phe293 (25). However, the results obtained were contrary to a previous study, thus indicating that the S-protein is likely to have a potential allosteric site that could prevent the interaction of the spike protein

with the host cell receptor.

PDB ID: 6M71 is the RNA-dependent RNA polymerase (RdRp) with a cofactor nsp12. The primary protein catalyzes the viral RNA replication and transcription process. Therefore, inhibiting this enzyme will suppress viral replication and further infection (26). The protein is comprised of several domains, including the N-terminal domain (1-397), finger domain (397-581 and 629-687), the palm region (582-628 and 688-815) and the thumb region (816-596) (27). The docking analysis revealed that christanoate has a higher affinity towards the active residues, which is similar to Remdesivir reported by Alizadehmohajer et al., (26) involving Lys47, His133, Asp135, Ala706, Ser709, Thr710, Gly774, Lys780 and Ser784 via hydrophobic contact in christanoate. Their study mentioned that the residues interacted with would establish an environment cohesive and stable upon forming the complex.

The study revealed that christanoate displayed higher affinity towards the proteins' docked with it of the two compounds analyzed. The long chain structure with one hydroxyl group and ester group played a crucial role in forming a stable complex, thus enhancing the inhibition activity. Comparably, favipiravir contains one hydroxyl group contributing to the hydrogen bond formed with the catalytic residues. Besides that, the amide and amino group in its structure was also observed to make much more stable hydrogen bonding with the proteins observed. Potential inhibitors of SARS-CoV viral proteins may disrupt the activity not just by responding to the catalytic site or the major active site but also by blocking the entry of the virus into the host cells. Inhibitors may achieve this by binding to the active residues and altering the protein structure, which could block the viral receptors' interaction with the host cells. Apart from that, inhibitors could also halt the viral replication and transcription cycle by altering the protein structure upon binding (27,28). Based on the interaction of christanoate with the proteins used in this, it has potential to inhibit the SARS-CoV.

Conclusion

The study revealed the antiviral activity of two major compounds identified in *Christia vesper-tilionis* leaf against SARS-CoV-2 using various protein structures modelled based on the virus structure and genome. Molecular docking is a method that can preliminarily illustrate the conformational structure of the viral protein and the potential inhibitor complex. Based on the investigation, christanoate can be further analyzed for its antiviral activity using pre-clinical techniques to confirm its bioactivity against SARS-CoV-2.

Acknowledgement

The authors thank Dana Penyelidikan & Inovasi Mara (DPIM) 2021 with reference number MARA/DPIM MARA.600-6/4/3(56) for supporting this study.

References

1. Prasetyo, W. E., Purnomo, H., Sadrini, M., Wibowo, F. R., Firdaus, M., and Kusumaningsih, T. Identification of potential bioactive natural compounds from Indonesian medicinal plants against 3-chymotrypsin-like protease (3CLpro) of SARS-CoV-2: Molecular docking, ADME/T, molecular dynamic simulations, and DFT analysis. *Journal of Biomolecular Structure and Dynamics*, 41(10), (2023), 4467-4484.
2. Ghufuran, Mehreen, Mehran, U., Haider, A. K., Sabreen, G., Muhammad, A., Muhammad, S., Syed, Q. A., Syed, S. U. H., and Simona, B. In-silico lead druggable compounds identification against SARS COVID-19 main protease target from in-house, chembridge and zinc databases by structure-based virtual screening, molecular docking and molecular dynamics simulations. *Bioengineering*, 10(1), (2023), 100.
3. Chen, Y., Guo, Y., Pan, Y., and Zhao, Z. J. Structure analysis of the receptor binding of 2019-nCoV. *Biochemical and Biophysical Research Communications*, 525(1), (2020), 135-140.

4. Tzenios, N., Chahine, M., and Tazanios, M. Better strategies for Coronavirus (COVID-19) vaccination. *Special Journal of the Medical Academy and Other Life Sciences*, 1(2), (2023).
5. Sofi, F., Dinu, M., Reboldi, G., Stracci, F., Pedretti, R.F., Valente, S., Gensini, G., Gibson, C.M. and Ambrosio, G. Worldwide differences of hospitalization for ST-segment elevation myocardial infarction during COVID-19: A systematic review and meta-analysis. *International Journal of Cardiology*, 3472022, (2022), 89-96.
6. Xue, Y., Husheng, M., Yisa, C., James, D. G., Qingsong, L., Ellen, W., and Jing, Y. Repurposing clinically available drugs and therapies for pathogenic targets to combat SARS-CoV-2. *MedComm*, 4(3), (2023), e2
7. Zheng, S., Fan, J., Yu, F., Feng, B., Lou, B., Zou, Q., Xie, G., Lin, S., Wang, R., Yang, X. and Chen, W. Viral load dynamics and disease severity in patients infected with SARS-CoV-2 in Zhejiang province, China, January-March 2020: Retrospective cohort study. *BMJ*, (2020), 369.
8. Agarwal, S., and Agarwal, S. K. Endocrine changes in SARS-CoV-2 patients and lessons from SARS-CoV. *Postgraduate Medical Journal*, 96(1137), (2020), 412-416.
9. Lee, J. J., Saiful, Y. L., Kassim, N. K., Che, A. C. A., Esa, N., Lim, P.C., and Tan, D.C. Cytotoxic activity of *Christia vespertilionis* root and leaf extracts and fractions against breast cancer cell lines. *Molecules*, 25(11), (2020), 2610.
10. Bunawan, H., Bunawan, S. N., and Baharum, S. N. The red butterfly wing (*Christia vespertilionis*): A promising cancer cure in Malaysia. *International Journal of Pharmacy and Pharmaceutical Sciences*, 7(8), (2015), 5.
11. Murugesu, S., Perumal, V., Balan, T., Fatinathan, S., Khatib, A., Arifin, N. J., Shukri, N. S. S. M., Saleh, M. S. and Hin, L. W. The investigation of antioxidant and anti-diabetic activities of *Christia vespertilionis* leaves extracts. *South African Journal of Botany*, 133, (2020), 227-235.
12. Wu, X. Y., Tang, A. C. and Lu, Q. Y. Study on antitumor effect of the extract from *Christia vespertilionis* in vivo. *Chinese Journal of Experimental Traditional Medical Formulae*, 8, (2012), 202-204.
13. Upadhyay, H. C., Sisodia, B. S., Cheema, H. S., Agrawal, J., Pal, A., Darokar, M. P. and Srivastava, S. K. Novel antiplasmodial agents from *Christia vespertilionis*. *Natural Product Communications*, 8(11), (2013), 1934578X1300801123.
14. Dash, G. K. An appraisal of *Christia vespertilionis* (LF) bakh. F.: A promising medicinal plant. *International Journal of Pharmacognosy and Phytochemical Research*, 8(6), (2016), 1037-1039.
15. Wang, M. Y., Zhao, R., Gao, L. J., Gao, X. F., Wang, D. P., and Cao, J. M. SARS-CoV-2: structure, biology, and structure-based therapeutics development. *Frontiers In Cellular And Infection Microbiology*, 10, (2020), 587269.
16. Hwang, W. C., Lin, Y., Santelli, E., Sui, J., Jaroszewski, L., Stec, B., and Liddington, R. C. Structural basis of neutralization by a human anti-severe acute respiratory syndrome spike protein antibody, 80R. *Journal of Biological Chemistry*, 281(45), (2006), 34610-34616.
17. Mycroft-West, C., Su, D., Elli, S., Li, Y., Guimond, S., Miller, G., and Skidmore, M. The 2019 Coronavirus (SARS-CoV-2) surface protein (spike) s1 receptor binding domain undergoes conformational change upon heparin binding. *BioRxiv*. (2020), 2020-02.
18. Liang, R., Wang, L., Zhang, N., Deng, X., Su, M., Su, Y., ... and Yu, F. Development of small-molecule MERS-CoV inhibi-

- tors. *Viruses*, 10(12), (2018), 721.
19. Khaerunnisa, S., Kurniawan, H., Awaluddin, R., Suhartati, S., and Soetjipto, S. Potential inhibitor of COVID-19 main protease (Mpro) from several medicinal plant compounds by molecular docking study. *Preprints*, (2020), 2020030226.
 20. Paasche, A., Zipper, A., Schäfer, S., Ziebuhr, J., Schirmeister, T., and Engels, B. Evidence for substrate binding-induced zwitterion formation in the catalytic Cys-His dyad of the SARS-CoV main protease. *Biochemistry*, 53(37), (2014), 5930-5946.
 21. Günther, S., Reinke, P. Y., Fernández-García, Y., Lieske, J., Lane, T. J., Ginn, H. M., ... and Meents, A. X-ray screening identifies active site and allosteric inhibitors of SARS-CoV-2 main protease. *Science*, 372(6542), (2021), 642-646.
 22. Sisakht, M., Mahmoodzadeh, A., and Darabian, M. Plant-derived chemicals as potential inhibitors of SARS-CoV-2 main protease (6LU7), a virtual screening study. *Phytotherapy Research*, 35(6), (2021), 3262-3274.
 23. Sharbidre, A., Dhage, P., Duggal, H., and Meshram, R. In silico investigation of *Tridax procumbens* phyto-constituents against SARS-CoV-2 infection. *Biointerface Research in Applied Chemistry*, 11, (2021), 12120-12148
 24. Pal, S., and Talukdar, A. Compilation of potential protein targets for SARS-CoV-2: Preparation of homology model and active site determination for future rational antiviral design. (2020).
 25. Khandelwal, A., and Sharma, T. Computational screening of phytochemicals from medicinal plants as COVID-19 inhibitors. (2020)
 26. Alizadehmohajer, N., Behmardi, A., Najafgholian, S., Moradi, S., Mohammadi, F., Nedaeinia, R., ... and Manian, M. Screening of potential inhibitors of COVID-19 with repurposing approach via molecular docking. *Network Modeling Analysis in Health Informatics and Bioinformatics*, 11(1), (2022), 1-11.
 27. Gao, Y., Yan, L., Huang, Y., Liu, F., Zhao, Y., Cao, L., Wang, T., Sun, Q., Ming, Z., Zhang, L., Ge, J., Zheng, L., Zhang, Y., Wang, H., Zhu, Y., Zhu, C., Hu, T., Hua, T., Zhang, B., Yang, X., Li, J., Yang, H., Liu, Z., Xu, W., Guddat, L. W., Wang, Q., Lou, Z., and Rao, Z. Structure of the RNA-dependent RNA polymerase from COVID-19 virus. *Science*, (2020), 779-782.
 28. Jakovac, H. COVID-19 and vitamin D—Is there a link and an opportunity for intervention? *American Journal of Physiology-Endocrinology and Metabolism*. (2020).
 29. Quartuccio, L., Sonaglia, A., McGonagle, D., Fabris, M., Peghin, M., Pecori, D., ... and Tascini, C. Profiling Covid-19 pneumonia progressing into the cytokine storm syndrome: Results from a single Italian Centre study on tocilizumab versus standard of care. *Journal of Clinical Virology*, 129, (2020), 104444.